Tabet, L. ; Bussy, C. ; Amara, N. ; Setyan, A. ; Grodet, A. ;Rossi, M.J. ; Pairon, J.C.K Boczkowski, J.K. and Lanone, S. Adverse effects of industrial multi-walled carbon nanotubes on human pulmonary cells. **Journal of Toxicology and Environmental Health. Part A** 2009, 72(2) :60-73.

Postprint version	Final draft post-refereeing
Journal website	http://www.tandf.co.uk/journals/titles/15287394.asp
Pubmed link	http://www.ncbi.nlm.nih.gov/pubmed/19034795
DOI	10.1080/15287390802476991

Adverse effects of industrial multi-walled carbon nanotubes on human pulmonary cells.

by

Lyes Tabet[1], Cyrill Bussy[1], Nadia Amara[1], Ari Setyan[2], Alain Grodet[3], Michel J. Rossi[4], Jean-Claude Pairon[5], Jorge Boczkowski[1,6], Sophie Lanone[1]

[1]INSERM, Unité 700, Paris, France; Université Paris 7, Faculté de Médecine, site X. Bichat, Paris, France

[2] Institut universitaire romand de Santé au Travail (Institute for Work and Health), Université de Lausanne et Université de Genève, Rue du Bugnon 21, CH-1005 Lausanne, Suisse

[3] INSERM, Unité 773, CRB3, Paris, France; Université Paris 7, Faculté de Médecine, site X. Bichat, Paris, France

[4]EPFL (Ecole Polytechnique Fédérale de Lausanne), LPAS (Laboratoire de Pollution Atmosphérique et Sol), Station 6, CH-1015 Lausanne, Suisse

[5] INSERM, Unité 841, Creteil, F-94010, France; Universite Paris 12, Faculte de Medecine, Creteil, F-94010, France; CHI Creteil, Service pneumologie et pathologie professionnelle, Creteil, F-94010, France

[6] Assistance Publique-Hôpitaux de Paris, Hôpital Bichat, CIC 007, Paris, France

Corresponding author

Jorge Boczkowski
Inserm U700
Faculté de Médecine Paris 7, site X. Bichat
BP416, 75870 Paris Cedex 18
FRANCE
Phone: (33 1) 57277584
Fax: (33 1) 57277541
E-mail: jorge.boczkowski@inserm.fr

Running head: Toxic effects of industrial carbon nanotubes

Abstract

The aim of this study was to evaluate adverse effects of multi-walled carbon nanotubes (MWCNT) produced for industrial purposes, on the human epithelial cell line A549. MWCNT were dispersed in dipalmitoyl lecithin (DPL), a component of pulmonary surfactant, and the effects of dispersion in DPL were compared to those in 2 other media: ethanol (EtOH) and phosphate buffer saline (PBS). Effects of MWCNT were also compared to those of 2 asbestos fibers (chrysotile and crocidolite) and carbon black (CB) nanoparticles, not only in A549 cells, but also on mesothelial cells (MeT5A human cell line), used as an asbestos-sensitive cell type. MWCNT formed agglomerates on top of both cell lines (surface area 15-35 μm^2), that were significantly larger and more numerous in PBS than in EtOH and DPL. Whatever the dispersion media, incubation with 100 μg/ml MWCNT induced a similar decrease in metabolic activity without changing cell membrane permeability or apoptosis. Neither MWCNT cellular internalization nor oxidative stress were observed. In contrast, asbestos fibers penetrated into the cells, decreased metabolic activity but not cell membrane permeability and increased apoptosis, without decreasing cell number. CB was internalized without any adverse effects.

In conclusion, this study demonstrates that MWCNT produced for industrial purposes exert adverse effects without being internalized by human epithelial and mesothelial pulmonary cell lines.

Introduction

Carbon nanotubes (CNT) are cylinders of one or several (up to 20) graphite layer(s) (single- or multi-wall carbon nanotubes respectively – SWCNT and MWCNT). Their diameter is in the order of the nanometer, and they can measure up to several micrometers in length. Because of their unique electrical properties, unusual strength and particular effectiveness in heat conduction, CNT are particularly promising nanomaterials for industrial use in medical as well as non-medical applications [see http://www.nanotechproject.org/44/ for inventory). However, the same novel properties that make CNT interesting raise concerns about their potential adverse effects on biological systems, which may lead to health issues.

Pulmonary effects of CNT have been evaluated in a number of *in vivo* and *in vitro* studies. Mice and rats exposed by the respiratory route showed acute and chronic pulmonary inflammation with and without fibrosis (Lam et al. 2004; Li et al. 2007; Muller et al. 2005; Shvedova et al. 2005; Warheit et al. 2004). Extra-pulmonary effects of respiratory administered CNT were also recently reported, with the presence of aortic mitochondrial DNA damage after a single intrapharyngeal installation of mice to SWCNTs (Li et al. 2007). Interestingly, a study by Shvedova *et al*. (2005) found the number of alveolar type II cells increased in response to SWCNT, which highlights the importance of this cell type in the pulmonary response to CNT exposure. *In vitro* studies demonstrated that CNT induced cytotoxicity and/or inflammatory responses in different cell types (Bottini et al. 2006; Cui et al. 2005; Ding et al. 2005; Jia et al. 2005; Kagan et al. 2006; Kisin et al. 2007; Manna et al. 2005; Monteiro-Riviere, Nemanich et al. 2005; Monteiro-Riviere, Inman et al. 2005; Sayes et al. 2006; Tian et al. 2006). However, among these studies, very few examined the effects of CNT on alveolar type II cells.

Accumulating evidence shows that adverse effects of CNT, as well as those of other nanomaterials, are related to their physico-chemical properties (Smart et al. 2006). Therefore,

effects observed with one CNT may not necessarily be extrapolated to another CNT, even if both are single or multi-walled. In this context, and from a public health perspective, it is critical to analyze potential adverse effects of CNT produced in large amounts for industrial applications. Indeed, although providing valuable information, several of the published studies investigated the effects of CNT produced in limited amounts in research lab for academic purposes. Other studies investigated the effects of CNT produced by small industrial companies, but further modified in research lab. All of these CNT might differ physically and chemically from the ones produced in large amounts for different industrial applications.

Therefore, the aim of the present study was to evaluate adverse effects of MWCNT produced for industrial purposes. These CNT were produced by chemical vapor deposition (CVD) in a French facility (ARKEMA France). Toxicological effects (cell viability, apoptosis and oxidative stress) as well as cellular internalization of CNT were analyzed in the human lung epithelial cell line A549, as representative of human alveolar type II cells (Foster et al. 1998).

To be as close as possible from the human respiratory exposure, MWCNT were dispersed in dipalmitoyl lecithin (DPL), a component of pulmonary surfactant (Lu et al. 1994). Since the dispersion status affects biological effects of nanomaterials (Monteiro-Riviere, Inman et al. 2005), the effects of dispersion in DPL were compared with those of dispersion in 2 other media: phosphate buffered saline (PBS) or ethanol (EtOH).

Concern exists about whether fiber-shaped nanoscale particles formed from carbon and other materials behave like asbestos, a toxic and carcinogenic fiber (Mohr, Keith, and Rihn 2005; Takagi et al. 2008; Poland et al. 2008). Therefore, in the present study, effects of MWCNT were compared to those of 2 asbestos fibers, chrysotile and crocidolite, as well carbon black (CB) nanoparticles. This comparison was performed not only using A549 cells, but also in mesothelial cells (human MeT5A cell line), which are sensitive to asbestos fibers (Mohr,

Keith, and Rihn 2005; Nymark et al. 2007).

METHODS

Experimental design

When intending to evaluate the potential adverse effects of nanomaterials, it is of prime importance to get a thorough knowledge of the nanomaterials that are used. Therefore, a thorough physico-chemical characterization of MWCNT (in powder, in solution and after contact with cells) was performed, using electronic microscopy techniques, and chemical analytic tools. In order to evaluate the potential adverse effects of nanomaterials, a comprehensive approach was used, aimed to evaluate both cytotoxic effects as well as the underpinning mechanisms (apoptosis, proliferation, oxidative stress, internalization).

Particles

MWCNT (Graphistrength C100, ARKEMA, France) were produced by CVD on a supported catalyst in a fluidized bed. Graphistrength C100 is produced as material composed of MWCNT entangled around the supported catalyst. These spherical heaps of MWCNT are about few 100 µm diameter and form a free flowing powder.

The effects of MWCNT were compared to those of 2 types of asbestos fibers; chrysotile (20-nm diameter) and crocidolite (80-nm diameter), from UICC (Union Internationale Contre le Cancer) (Kido et al. 2008; Dopp et al. 1997); and nanosized carbon black (CB, FR101, primary particles of 95-nm diameter; Degussa/Evonik, Germany - Pigmentrusse/pigment blacks, Technische Daten Europa/Technical Data Europe, Degussa AG, Advanced Fillers & Pigments, 2006).

CNT physico-chemical characterization

MWCNT dimensions were measured by Transmission Electron Microscopy (TEM).

Chemical composition and carbon content were determined by inductively coupled plasma spectroscopy (ICP-MS), electron spectroscopy for chemical analysis (ESCA), scanning Electron Microscopy (SEM) and TEM analysis (Figure 1A). Specific surface area was measured using Brunauer Emmett Teller (BET) method using adsorption isotherms of nitrogen at 77K. The surface composition in terms of functional groups was examined by surface titration using 6 probe gases undergoing heterogeneous reactions in a Knudsen flow reactor (Demirdjian and Rossi, 2005).

Particle suspensions

MWCNT were suspended at 10 mg/ml in aqueous DPL, PBS or EtOH. Asbestos fibers were suspended in culture medium, and CB particles in PBS. Particle solutions were vortexed for 1 min, sonicated (RLI 275 sonication bath, LIREC, France) for 30 min under cooling conditions, with 30-sec interruption every 10 min for vortex at maximum speed. Immediately after the end of sonication, particle solutions were vortexed for 1 min at maximum speed and diluted in culture medium. The particle size distribution function (PSD) of the different particle suspensions were analyzed using a Malvern Mastersizer S and were represented by the volume distribution functions in the range 50 nm to 880 μm. For these experiments, particles have also been suspended in pure H_2O as a control. As usual, the results have been analyzed using the spherical particle approximation with refractive indices of 1.5295 and 1.3300 for CNT and H_2O, respectively. The measurement of the PSD in the submicron range in terms of a number rather than volume distribution has been attempted using a SMPS system (TSI Inc.) in which the particle suspension has been atomized after suitable sonication. However, the solvent blanks already resulted in several 10^4 counts in the 20 to 200 nm diameter range, presumably owing to solutes giving rise to aerosol particles after evaporation of H_2O, so that this effort had to be abandoned.

The formation of agglomerates in suspension was characterized by TEM analysis. An aliquot of solutions was deposited on 47mm diameter polycarbonate filters (0.2 μm pores) and further analyzed by TEM with a JEOL 1200 EX II microscope (Figure 1B). In addition, agglomerates formation after cell incubation with particles was measured by optical microscopy (see below).

Cell culture and stimulation

Human alveolar epithelial cells (A549 cell line, ATCC, France) and mesothelial cells (MeT5A cell line, ATCC, France) were cultured as previously described (Amara et al. 2007; Nymark et al. 2007), seeded in 96-well plates at 60 000 cells/ml and grown to confluence (48 to 72 hr later). Cells were exposed for 6, 24, 48 or 72 hr to serum-free medium, 0.1 to 100 μg/ml (0.02-20 μg/cm^2) of MWCNT, or 100 μg/ml (20 μg/cm^2) asbestos fibers or CB nanoparticles. The final concentration of DPL, PBS, or EtOH in the culture medium was 1% for each condition of stimulation, a concentration that did not elicit any cell toxicity (data not shown). As MeT5A cells were used only to verify the main results obtained with A549 cells, these cells were exposed only to DPL-suspended MWCNT at different concentrations (0.1 to 100 μg/ml).

Assessment of cell morphology and agglomerates formation after cell incubation with particles

Cell morphology was assessed by optical microscopy in cells stained with Harris hematoxylin-phloxin. During the observations, it was noted that MWCNT appeared as agglomerates attached to cells. These agglomerates were further quantified in A549 and MeT5A cells exposed for 48 hr to 100 μg/ml MWCNT suspended in different media. For each condition of stimulation, 10 fields (magnification 10 x) were selected from the top to the

bottom across the vertical diameter of the culture well. The following parameters were analyzed by use of a video microscope coupled to the AnalySIS® 3.0 software (Soft Imaging System GmbH, Germany): *1)* proportion of the field surface occupied by cells, *2)* number of agglomerates present in each examined field, and *3)* surface area of each agglomerate. An agglomerate was defined as a black individualized area, of more than 0.20 μm^2. Analysis was performed blinded by 2 independent observers (LT and NA). The coefficient of variation for measurement of the 3 parameters was <5%.

Assessment of cell viability

Two methods were used to evaluate changes in cell viability: MTT, and Neutral Red assays. These tests were performed as previously described (Davoren et al. 2007; Monteiro-Riviere, Nemanich et al. 2005; Monteiro-Riviere, Inman et al. 2005; Worle-Knirsch, Pulskamp, and Krug 2006). Results of cell viability are expressed as the means of at least 3 independent experiments, each of 6 replicates, given as the ratio of the mean for each condition to the mean of the control condition (cells cultured in media containing the respective suspension agent). Since nanomaterials might interfere with cytotoxicity tests (Monteiro-Riviere and Inman 2006; Worle-Knirsch, Pulskamp, and Krug 2006), the assays were performed with and without 100 μg/ml MWCNT during incubation with the dye and measured absorbance. No interference of MWCNT with MTT and Neutral Red assays was observed (data not shown).

Assessment of cell number

Cell number was assessed by quantifying DNA content with the fluorescent dye bisbenzimide H33258 (Hoechst 33258, Sigma, France). The dye was added to cells at the end of the stimulation period (24, 48 or 72 hr) and fluorescence was measured at 460 nm (excitation: 360 nm). Interference of MWCNT with the fluorescent dye was evaluated by the incubation

of a known concentration of DNA in presence or absence of 100 μg/ml of MWCNT. No interference was observed (data not shown).

Assessment of apoptosis

- *DAPI staining*

Apoptosis was examined by 4',6-diamidino-2-phenylindole dihydrochloride (DAPI) staining (Sigma-Aldrich, France) coupled to fluorescence microscopy analysis in the same experimental setting than used for assessment of cell number. Cells were seeded onto sonic seals and were exposed for 24, 48 or 72 hr to 100 μg/ml of particles or suspension medium alone. At the end of stimulation, the cells were fixed with 4% paraformaldehyde in PBS for 25 min at room temperature. DAPI solution (1 μg/ml) was added for 5 min at 37°C. Observations involved use of a fluorescence video microscope (Leica DMIRB) (excitation 358 nm; emission 461 nm). For each condition of stimulation, 10 fields (magnification 63 x) were selected from top to bottom across the vertical diameter of the culture well. The % of apoptotic cells was calculated as follows: % of apoptotic cells = (total number of cells with apoptotic nuclei/total number of counted cells) x 100. Analysis was performed in a blind way by 2 independent observers (LT and NA). The coefficient of variation for measurement of the 2 parameters was <5%.

- *DNA laddering*

Genomic DNA (250ng) of cells exposed for 72 hr to DPL 1% or 100 μg/ml MWCNT, crocidolite or etoposide as a positive control was extracted and purified using DNAeasy Blood & Tissue QIAGEN kit (Qiagen, France) as per the manufacturer's instructions. Finally, degradation of DNA was visualized with SYBR Green on a 1.5% agarose gel.

Assessment of cell proliferation

The effects of nanomaterials on cell proliferation were determined by the bromodeoxyuridine (BrdU) cell proliferation ELISA (Roche applied science, Germany). The assay is based on the immunodetection of BrdU incorporated into the genomic DNA in place of thymidine of proliferating cells.

Cells were cultured in 96-well plates. Upon confluence, they were exposed, in serum-free medium, for 24, 48 or 72 hr to particles from 0.1 to 100 μg/ml or to suspension medium alone. BrdU was added to the medium 20 hr before the end of stimulation. At the end of incubation, the labeling solution was removed, and 200 μl of FixDenat solution was added and incubated for 30 min at room temperature. After removing FixDenat, 100 μl of anti–BrdU-POD solution was added and incubated for 90 min at room temperature. After washing three times with 200 μl/well of washing buffer, the 100 μl of tetramethylbenzidine (TMB) substrate solution was added and incubated for 5 to 30 min at room temperature until color development was sufficient for photometric detection. The reaction was stopped with the addition of 25μl/well of H_2SO_4 (1M). The absorbance of the samples was measured in a microplate reader at 450-690 nm within 5 min after adding H_2SO_4.

Assessment of internalization of nanomaterials

Cells exposed for 48 hr to different nanomaterials at 100 μg/ml were analyzed by Transmission Electronic Microscopy (TEM). Cells were adherent on their plastic surface and fixed *in situ* or were trypsinized and fixed in suspension in a mix of 2% paraformaldehyde – 0.5% glutaraldehyde, post-fixed in 1% osmic acid and embedded in Epon. Fine (1-μm thick) and ultra-fine (60-nm thick) slices were cut, stained with uranyl acetate and lead salt, and observed under Jeol 1010 TEM (60 keV). As observations were similar after both fixation processes (*in situ* or after trypsinization) only *in situ*-fixed cells are shown.

Markers of oxidative stress

Oxidative stress was evaluated by analyzing mRNA expression of the anti- and pro-oxidant systems HO-1, SOD2, GPx and NOX4 respectively (Amara et al. 2007; Ryter and Choi 2005; Sumimoto, Miyano, and Takeya 2005) by quantitative real-time RT-PCR by use of the PCR ABI 7700 apparatus (Applied Biosystems), after exposure of cells for 6 or 24 hr up to 100μg/ml nanoparticles. The following sets of primers were used: HO-1, 5'-TTCTTCACCTTCCCCAACATTG-3' and 5'-CAGCTCCTGCAACTCCTCAAA-3', SOD2 5'-GAACGAGCATCCTGTCTTCG-3' and 5'-CCAAATGATGAGCTTGGGATC-3', GPX-2 5'-GCCCTGGAACCTCACATCAAC-3' and 5'-CGGCTCAGGTTGTTCACGTAG-3', and NOX4, 5'-CTCAGCGGAATCAATCAGCTGTG-3' and 5'-AGAGGAACA CGACAATCAGCCTTAG-3. Ubiquitin was used as house-keeping gene: 5'-CACTTGGTCCTGCGCTTGA-3' and 5'-TTTTTTGGGAATGCAACAACTTT-3'. Expression of mRNA was normalized to that of ubiquitin. In previous experiments it was verified that ubiquitin mRNA expression did not change in the different experimental conditions (data not shown).

Statistical analysis

Experiments were performed at least in triplicate. Values are given as mean S.E.M of values obtained for each experiment. The data were analyzed by non-parametric tests (GraphPad Prism software). A $p<0.05$ was considered significant.

RESULTS

Physico-chemical characteristics of CNT

MWCNT present an average diameter of 12 nm (size distribution: 0-15 nm; 85%, 15-30 nm;

13%, and >30 nm; 2%) and a length of 0.1 up to 13 μm as observed by TEM (Figure 1A). No free amorphous carbon was detectable by SEM and TEM, and ESCA revealed the presence of graphitic carbon, with only 0.8 at% of oxygen. Metallic impurities, measured by ICP-MS, were aluminum 2.4% and iron 2%. BET analysis under nitrogen gave a specific surface area value of 219.2 m^2/g.

Surface chemical analysis of MWCNT was based on titration of surface functional groups using 6 probe gases ($N(CH_3)_3$, NH_2OH, HCl, CF_3COOH, O_3, NO_2) that specifically interacted with the MWCNT sample located in the sample compartment of a Knudsen flow reactor. Table 1 indicates the number of functional groups located on the surface of MWCNT that are "interrogated" by the probe gases per mg and per cm^2 of MWCNT or in terms of a formal monolayer of probe gas adsorbed on MWCNT. As an example, the base $N(CH_3)_3$ interacts with acidic surface groups. Four main conclusions may be drawn from the results displayed in Table 1: (i) there are very few acidic sites interacting with $N(CH_3)_3$, significantly less than on Diesel soot (Setyan, personal communication); (ii) the degree of partial oxidation of MWCNT, that is the amount of carbonyl groups interacting with NH_2OH, is comparable to commercially available amorphous carbons such as CB, but smaller than for Diesel soot or secondary organic aerosol (SOA) (Setyan, personal communication), which indicates a moderate degree of surface oxidation; (iii) there is a high degree of unsaturation present on the surface as measured by O_3 uptake, which may be due either to the presence of olefinic double bonds or polycyclic aromatic hydrocarbon moieties with double bond localization such as acenaphthylene, pentalene or azulene; (iv) the surface of MWCNT is multifunctional indicating apparent coexistence of acidic and basic sites as well as partially oxidized and reduced (unsaturated) sites on the surface of MWCNT without apparent internal acid-base or redox reactions.

Particle agglomerate formation in suspension and over exposed cells

The results of the PSD measurement of the suspensions using light scattering may be summarized as follows: none of the suspensions (pure bidistilled H_2O, 1% DPL, 1% EtOH, 1% PBS) showed the presence of primary particles of CNT, undoubtedly owing to lack of sensitivity of the instrument. However, after sonication, the suspensions in pure H_2O and 1% EtOH showed the presence of submicron particles with a volume fraction of 13.6 and 2.5% integrated around the maximum at 60 ± 5 nm which corresponds to the presence of 10^9 and 2.5 x 10^{10} submicron particles of 60 nm to one particle at 100 and 650 μm, respectively. The sensitivity of the used instrument is apparently not sufficient to detect the volume fraction of the primary CNT particles in the suspensions of DPL and PBS, even after sonication. Interestingly enough, the presence of the additives seems to affect primarily the size of the agglomerates whose size changes upon sonication except in suspensions containing 1% DPL. The latter is characterized by a significant volume fraction of heavy particles at 22.5 and 480 μm, frequently detectable even by the naked eye. Based on the sonication experiments we expect a large number of primary CNT particles even in this case.

Transmission Electron Microscopy (TEM)

As shown in Figure 1B, MWCNT form agglomerates that either preexisted in solution, irrespective of the dispersion media, or that were generated during solvent evaporation in the course of the preparation of the TEM sample. Moreover, individual MWCNT less than 100 nm in dimension can also be observed in all 3 media. This diameter from TEM imaging is commensurate with the MWCNT monomer, that is primary particle diameter from light scattering experiments (see above).

Optical microscopy

Optical microscopy examination of cells exposed to 100 μg/ml MWCNT, asbestos or CB nanoparticles for 48 hr revealed no change in the morphology of exposed cells. Control and exposed A549 cells showed typical cuboidal shape, indicative of type II alveolar cell morphology (Figure 2A) (Nardone and Andrews 1979), and MeT5A cells showed typical features of mesothelial cells (Figure 2B) (Mutsaers 2004). MWCNT formed agglomerates (black area on the field), which seem to be on the top of the cells, because they strictly co-localized with the cells despite thorough washing before the fixation/staining procedure. Exposure of A549 cells to 3 different suspensions of MWCNT led to formation of agglomerates (range 15 to 30 μm^2) that were significantly larger in PBS than in DPL and EtOH (Table 2). The results from inspection of optical microscopy images displayed in Table 2 are in rough qualitative agreement with the PSD obtained in MWCNT suspensions despite the very disparate nature of the experiments. Light scattering resulted in apparent diameters of 22.5, 21 and 100 μm for DPL, EtOH and PBS-containing suspensions of MWCNT, respectively. In this comparison, the largest particles recorded in the course of light-scattering experiments were omitted owing to their rarefaction in terms of number concentration compared to the large number of smaller particles. The mean number of agglomerates was significantly lower when MWCNT were dispersed in EtOH than in the 2 other media ($p<0.05$, Table 2). The fraction of the field surface occupied by cells did not vary with the different experimental conditions (data not shown). The size of agglomerates formed by MWCNT suspended in DPL was similar over A549 and MeT5A cells. However, the number of agglomerates appeared less important in MeT5A cells.

Cell viability

Cell viability was analyzed with the MTT and Neutral Red assays, which determine mitochondrial metabolism and plasma membrane permeability respectively. For the MTT

assay, MWCNT effects on A549 cell viability were similar for the 3 dispersion media (Figure 3A). Compared with respective controls (cells cultured in media containing the respective suspension agent without particles), MTT values decreased significantly with 10 μg/ml to 100 μg/ml incubation, reaching 60% of control values for 100 μg/ml incubation at 48 hr post-exposure (for 10 and 100 μg/ml). Similar results were obtained after exposure of MeT5A cells to DPL-suspended MWCNT (Figure 3B and data not shown – for a better reading, only results obtained after 48 hr incubation of MeT5A cells with the different nanoparticles are shown subsequently). In both cell types, incubation with 100 μg/ml chrysotile or crocidolite elicited similar decreases in MTT, which were not different from that induced by 100 μg/ml MWCNT after 24 hr. No change in MTT was observed when cells were incubated with CB nanoparticles at 100 μg/ml, except for significant decrease after incubation of MeT5A cells with CB for 48 or 72 hr (Figure 3).

In contrast, results of the Neutral Red assay showed no significant alteration of A549 cell viability after incubation with MWCNT in the 3 media, whatever the time point considered (data not shown). Similar results were observed with MeT5A cells (data not shown). Moreover, neither asbestos fibers nor CB nanoparticles induced significant diminution of viability as assessed by Neutral Red assay, whatever the cell type studied (data not shown). Interestingly, incubation of both cell types with asbestos fibers induced an increase in Neutral Red incorporation, as well as incubation of MeT5A cells with CB nanoparticles for 6 or 24 hr (data not shown). Collectively, these results suggest that MWCNT and asbestos fibers alter mitochondrial metabolism, with no apparent effect on cell membrane permeability.

Cell number, apoptosis and proliferation

Whether the impaired mitochondrial metabolism might result in decreased cell number after incubation with MWCNT was next evaluated. This was first assessed by quantifying DNA

content. Incubation with 100 μg/ml MWCNT resulted in a significant decrease in A549 cell number after 24, 48 and 72 hr regardless of dispersion media, with a reduction of 15 to 20% of control cell number (Figure 4A). No such effect was observed with MeT5A cells (Figure 4B and data not shown). Moreover, neither asbestos fibers nor CB induced a significant decrease in total DNA content, except after 24 hr treatment of MeT5A cells with CB (Figure 4 and data not shown). Furthermore, a significant increase in DNA content was observed after incubation of A549 cells with crocidolite for 48 hr.

To investigate the mechanism(s) involved in the reduced A549 cell number after MWCNT incubation, apoptosis was examined. DAPI staining showed a small proportion of control cells with apoptotic nuclei (1 to 2% of total cells) at 48 and 72 hr, and this fraction did not change significantly in the cells incubated with MWCNT (Figure 5 and data not shown). In contrast, a significant increase in the proportion of apoptotic cells was observed after 72 hr incubation with crocidolite (approximately 5% of total cells). Similar results were obtained with MeT5A cells (Figure 5 and data not shown). DNA laddering experiments confirmed those results in both cell types, except for an absence of modification induced by exposure to asbestos fibers (Fig. 6 and data not shown).

Finally, no significant modification of proliferation was observed, whatever the nanomaterials, type point and cell type (data not shown).

Cellular internalization of nanomaterials

Internalization of the different materials in A549 cells was analyzed by TEM, which showed morphological features such as lamellar body structure, microvilli and tonofilament characteristics of alveolar epithelial type II cells in control cell culture (Figure 7). These morphological characteristics were similar in cells incubated with 100 μg/ml MWCNT for 24 hr. No nuclear change revealing apoptosis was observed. No evidence of MWCNT

internalization, whatever the dispersion media used, was found. In contrast, CB particles and chrysotile and crocidolite fibers were observed inside cells incubated with these particles. Similar results were obtained after exposure of MeT5A cells to the different nanomaterials (data not shown).

Oxidative stress

Since MWCNT were not internalized in cells, whether the observed decrease in viability could be related to oxidative stress was examined by analyzing mRNA expression of the different genes implied in an oxidative response: HO-1, SOD2, GPx and NO-4 (Li and Shah 2002; Taille et al. 2004). No significant change in expression of HO-1 mRNA was observed in cells incubated with MWCNT in the different media for 6 or 24 hr or with asbestos fibers (data not shown). The same results were obtained for SOD2 and GPx genes (data not shown). Finally, no change was observed in the mRNA of NOX4 (data not shown), a pro-oxidant system involved in amplification of the oxidative response in cells exposed to diesel exhaust particles (Amara et al. 2007).

DISCUSSION

The MWCNT examined in the present study were produced by CVD as spherical sets of agglomerates of primary MWCNT particles in the range of several tens to several hundreds of micrometers of diameter. In the present study, the aim was to be as close as possible to an *in vivo* respiratory exposure and therefore the CNT were dispersed in DPL, a component of pulmonary surfactant. The issue of the biological relevance of dispersion media in the evaluation of the toxicological effects of manufactured nanomaterials is critical (Fu and Sun 2003; Monteiro-Riviere, Inman et al. 2005; Lanone and Boczkowski 2006) and DPL has been

extensively used in studies investigating the respiratory effects of air pollution particles (Bachoual et al. 2007; Baulig et al. 2003). Using this method of dispersion it was observed that, in addition to the presence of primary MWCNT particles, MWCNT agglomerates of micrometer size were present in solution based on TEM image analysis, light scattering of the suspension and optical microscopy of exposed cells. The relative contribution of the primary particles to the agglomerates is not known when the particles come out of production. Indeed, it is well documented that individual, raw CNT form agglomerates in solution. Dispersing the MWCNT in the 2 other examined media (PBS ad EtOH), resulted also in similar formation of agglomerates accompanied by the presence of primary MWCNT particles. Although agglomerates in DPL were smaller than in PBS, they were still in the μm range. In DPL two types of aggregates corresponding to a bimodal distribution of 22.5 and 480 μm peak diameter in terms of volume fraction, were observed, whereas in PBS a single broad particle distribution from 10 to 400 μm was recorded that may have coalesced from the bimodal PSD distribution function. It needs to be stressed however, that, irrespective of the dispersing media, not all the MWCNT present in the solution formed agglomerates, since individual CNT were observed by TEM analysis of the suspensions. Light scattering reveals a significant relative number concentration of primary MWCNT particles on the order of 10^8 to $2.5x10^{10}$ particles to one, thereby reaching volume fractions up to 13.6% at a modal diameter of 60 ± 5 nm in pure H_2O after sonication. Sonication experiments in 1% EtOH dispersant reveal the partly reversible nature of aggregation and break-up of the MWCNT aggregates into primary particles, but also the re-agglomeration with time once sonication has been halted.

Irrespective of the dispersing media, MWCNT induced a concentration- and time-dependent decrease in mitochondrial metabolism, as revealed by a significant decrease in MTT reduction, but no effect on membrane permeability, as revealed by Neutral Red assay. Gao et al. (Gao et al. 2001) showed that silica particles, when mixed with Dipalmitoyl

phosphatidylcholine (DPPC), lose their cytotoxic potential on NR8383 rat alveolar macrophages. However, in the same study, the authors also fail to demonstrate such protective effect of surfactant coating for kaolin particles. The absence of effect of dispersion in DPL, as compared to other media, on MWCNT-induced cytotoxicity is in agreement with data published by Monteiro-Riviere and collaborators (Monteiro-Riviere, Inman et al. 2005) and Wick and collaborators (Wick et al. 2007) showing that cytotoxicity of MWCNT in human epidermal keratinocytes and mesothelial cells was independent of their dispersion in different concentrations of surfactants. However, Monteiro-Riviere et al. showed that HEK cells exposed to CNT dispersed in surfactant produced less IL-8 than cells exposed to CNT alone (Monteiro-Riviere, Inman et al. 2005). Therefore, if dispersion in various media, and in surfactant in particular, is an important point to study, biological effects can't be considered as the results of one single end-point. An effect of MWCNT on mitochondrial metabolism without any alteration in cell membrane integrity, agrees with results published by different groups examining separately these parameters in A549 (Davoren et al. 2007) and other cell types (Muller et al. 2005; Wick et al. 2007). This could be explained by the different intracellular targets/mechanisms of the two assays. The metabolic effect of MWCNT on A549 cells further resulted in a decreased cell number after 48 to 72 hr incubation, as shown by decreased cellular DNA content, without any apoptosis or necrosis. The decrease in cell metabolism and number occurred essentially after 24 hr cell incubation with MWCNT and was stable thereafter, suggesting an initial, non-progressive insult. Despite a similar degree of metabolic effect of MWCNT on MeT5A cells, no decrease of total cell number was observed as well as any sign of apoptosis. Since in both cells types, no compensatory modification of proliferation has been observed, the exact mechanisms implied in these events still need to be discovered. A possibility could be a modification of cell architecture, as described by Kaiser et al. (Kaiser et al. 2008), that could induce subsequent modification in cell physiology,

specific to each cell type, or, as proposed by Fung et al. (Fung et al. 1997), differing repair capacities. However, these possibilities need further study.

MWCNT internalization in exposed cells was not seen. It is important to note, however, that while large agglomerates may not get internalized, small individual tubes could be (such as those identified by light scattering experiments reported earlier in this study) although they may not be visible at light microscopy level or even with TEM. Few studies have investigated the relation between agglomerate formation and CNT internalization. Monteiro-Riviere and coworkers (Monteiro-Riviere, Nemanich et al. 2005, Bussy et al. 2008) showed that the cytotoxic effect of MWCNT agglomerates to human epidermal keratinocytes resulted from CNT internalization. However, Davoren and coworkers (2007) found no SWCNT internalization in A549 cells, using a different solubilization media than utilized here. Wörle-Knirsch and colleagues (2006) found SWCNT present in A549 cells, but prior to cell exposure the CNT underwent an acidic treatment that may have modified surface reactivity (Fu and Sun 2003) and subsequent CNT internalization. Indeed, CNT uptake by cells is currently being discussed and might depend on the state of functionalization and morphology of the material (Bianco, Kostarelos, and Prato 2005). Collectively, our results and those of Davoren and coworkers (2007) suggest that CNT, either SW or MW, are not always internalized in A549 cells, despite their differing degrees of agglomeration. Some studies showed that, when comparing different aggregated nanomaterials, one can't conclude on the relative cytotoxicity induced by those materials from the agglomerate size range (Soto, Garza, and Murr 2007). Finally, another important issue is that internalization is not an end-point for particles to have a biological effect. Indeed, Ovrevik et al. (Ovrevik et al. 2006) showed that silica particles induce a cascade of events prior to any internalization of the particles in A549 cells. Therefore, the relationship between agglomeration and internalization, if very

interesting, is maybe not the only relevant parameter to understand biological effects of MWCNT.

The effect of our MWCNT on cell metabolism may rely on mechanisms other than cell internalization. In this context, occurrence of oxidative stress, postulated as a central mechanism in the cellular toxic effects of nanoparticles was explored (Nel et al. 2006), but expression of neither HO-1, a redox-sensitive antioxidant system, nor GPx or SOD in MWCNT-exposed A549 or MeT5A cells was modified. Furthermore, the expression of the pro-oxidant system NOX4, induced by diesel exhaust particles in A549 cells (Amara et al. 2007), was unchanged in these cells. Such results could be because of the cancerous nature of A549 cells, as cancer cell lines are known to be refractory to oxidant stress. However, along with exposure to particles, we exposed cells to hydrogen peroxide as a positive control for oxidative stress generation, and found an increase in oxidative stress markers (data not shown). Therefore, other non-oxidant mechanisms may also be important to the effects of MWCNT and asbestos. Activation of cell-surface receptors, involving a redox-independent signaling cascade may be an alternative explanation. Interestingly, Ovrevik and coworkers (2006) recently showed that silica upregulates IL-8 release from A549 cells through interactions with membrane components prior to particle internalization. However, such a mechanism might not occur in our study since, as opposed to silica, which is acidic, our industrially produced MWCNT present few acidic groups at their surface. The oxidable groups present at their surface could potentially act as free radicals scavengers, as shown by Fenoglio and collaborators (2006). However, investigation of such mechanisms requires further study.

As stated previously, data are scarce in the current literature comparing the effects of CNT with those of asbestos fibers. Wick and coworkers (2007) showed that agglomerates of CNT induced a similar cytotoxic effect as crocidolite fibers in the human mesothelioma cell line

MSTO-211H, but the ultrastructural and molecular basis underlying these effects were not established. A recent pilot study, by Poland and coworkers, also showed similar effects of carbon nanotubes and asbestos fibers in mice which mesothelial lining of the body cavity has been exposed, as a surrogate for the mesothelial lining of the chest cavity (Poland et al., 2008). However, the exact molecular pathways were not deply addressed. In the present study, although both MWCNT and asbestos fibers induced similar alterations in viability of A549 and MeT5A cells: *1)* in contrast to MWCNT, asbestos fibers did not diminish cell number but augmented apoptosis, and *2)* MWCNT were not internalized in cells whereas asbestos fibers were clearly internalized. The nature of the effects induced by MWCNT and asbestos fibers were different, although the present study can't give definitive answers on that issue.

In conclusion, this study shows that MWCNT produced by CVD for industrial purposes as spherical sets of several hundreds of microns exert adverse biological effects without being internalized by human epithelial and mesothelial pulmonary cells.

ACKNOWLEDGEMENTS

Lyes TABET is a recipient of a joint grant from ADEME (Agence de l'Environnement et de la Maitrîse de l'Énergie) and ARKEMA. Part of this work was supported by the French ANR through RESPINTTOX project (SEST program) and by the Région Ile-de-France in the frame-work of C'nano-IdF, NANOTUBTOX project. C'Nano-IdF is the nanoscience competence center of Paris Region, supported by CNRS, CEA, MESR, and Région Ile-de-France. Nadia Amara is supported by Chancellerie des Universités de Paris (legs Poix) and Jorge Boczkowski by INSERM and Assistance Publique-Hôpitaux de Paris (Contrat d'Interface). Authors would like to thank Marie-Annick Billon-Galland for her help and expertise in electronic microscopy, Marie-Claude Jaurand for providing the Met5A cells, and Hélène Desquerroux (ADEME) for her helpful comments. Ari Setyan and Michel J. Rossi would like to acknowledge partial support from the French NANOTOX (ANR) program.

BIBLIOGRAPHY

Amara, N., R. Bachoual, M. Desmard, S. Golda, C. Guichard, S. Lanone, M. Aubier, E. Ogier-Denis, and J. Boczkowski. 2007. Diesel Exhaust Particles Induce Matrix Metalloprotease-1 in Human Lung Epithelial Cells Via a Nadp(H) Oxidase/Nox4 Redox-Dependent Mechanism. *Am J Physiol Lung Cell Mol Physiol*.

Bachoual, R., J. Boczkowski, D. Goven, N. Amara, L. Tabet, D. On, V. Lecon-Malas, M. Aubier, and S. Lanone. 2007. Biological effects of particles from the paris subway system. *Chem Res Toxicol* 20 (10):1426-33.

Baulig, A., M. Sourdeval, M. Meyer, F. Marano, and A. Baeza-Squiban. 2003. Biological effects of atmospheric particles on human bronchial epithelial cells. Comparison with diesel exhaust particles. *Toxicol. Vitro* 17:567-573.

Bianco, A., K. Kostarelos, and M. Prato. 2005. Applications of carbon nanotubes in drug delivery. *Curr Opin Chem Biol* 9 (6):674-9.

Bottini, M., S. Bruckner, K. Nika, N. Bottini, S. Bellucci, A. Magrini, A. Bergamaschi, and T. Mustelin. 2006. Multi-walled carbon nanotubes induce T lymphocyte apoptosis. *Toxicol Lett* 160 (2):121-6.

Bussy, C., J. Cambedouzou, S. Lanone, E. Leccia, V. Heresanu, M. Pinault, M. Mayne-L'hermite, N. Brun, C. Mory, M. Cotte, J. Doucet, J. Boczkowski, and P. Launois. 2008. Carbon Nanotubes in Macrophages: Imaging and Chemical Analysis by X-ray Fluorescence Microscopy. *Nano Lett*.

Cui, D., F. Tian, C. Ozkan, M. Wang, and H. Gao. 2005. Effect of single wall carbon nanotubes on human HEK293 cells. *Toxicol. Letters* 155:73-85.

Davoren, M., E. Herzog, A. Casey, B. Cottineau, G. Chambers, H. J. Byrne, and F. M. Lyng. 2007. In vitro toxicity evaluation of single walled carbon nanotubes on human A549 lung cells. *Toxicol In Vitro* 21 (3):438-448.

Demirdjian, B. and M.J. Rossi (2005). “The surface properties of SOA from limonene and toluene using specific molecular probes: a new experimental technique”. Atmos. Chem. Phys. Discuss. **5**: 607-654.

Ding, L., J. Stilwell, T. Zhang, O. Elboudwarej, H. Jiang, J. P. Selegue, P. A. Cooke, J. W. Gray, and F. F. Chen. 2005. Molecular characterization of the cytotoxic mechanism of multiwall carbon nanotubes and nano-onions on human skin fibroblast. *Nano Lett* 5 (12):2448-64.

Dopp, E., M. Schuler, D. Schiffmann, and D. A. Eastmond. 1997. Induction of micronuclei, hyperdiploidy and chromosomal breakage affecting the centric/pericentric regions of chromosomes 1 and 9 in human amniotic fluid cells after treatment with asbestos and ceramic fibers. *Mutat Res* 377 (1):77-87.

Foster, K. A., C. G. Oster, M. M. Mayer, M. L. Avery, and K. L. Audus. 1998. Characterization of the A549 cell line as a type II pulmonary epithelial cell model for drug metabolism. *Exp Cell Res* 243 (2):359-66.

Fu, K., and Y. P. Sun. 2003. Dispersion and solubilization of carbon nanotubes. *J Nanosci Nanotechnol* 3 (5):351-64.

Fung, H., Y. W. Kow, B. Van Houten, and B. T. Mossman. 1997. Patterns of 8-hydroxydeoxyguanosine formation in DNA and indications of oxidative stress in rat and human pleural mesothelial cells after exposure to crocidolite asbestos. *Carcinogenesis* 18 (4):825-32.

Gao, N., M. J. Keane, T. Ong, J. Ye, W. E. Miller, and W. E. Wallace. 2001. Effects of phospholipid surfactant on apoptosis induction by respirable quartz and kaolin in NR8383 rat pulmonary macrophages. *Toxicol Appl Pharmacol* 175 (3):217-25.

Jia, G., H. Wang, L. Yan, X. Wang, R. Pei, T. Yan, Y. Zhao, and X. Guo. 2005. Cytotoxicity of carbon nanomaterials: single-wall nanotube, multi-wall nanotube, and fullerene. *Environ. Sci. Technol.* 39:1378-1383.

Kagan, V. E., Y. Y. Tyurina, V. A. Tyurin, N. V. Konduru, A. I. Potapovich, A. N. Osipov, E. R. Kisin, D. Schwegler-Berry, R. Mercer, V. Castranova, and A. A. Shvedova. 2006. Direct and indirect effects of single walled carbon nanotubes on RAW 264.7 macrophages: Role of iron. *Toxicol Lett* 165:88-100.

Kaiser, J. P., P. Wick, P. Manser, P. Spohn, and A. Bruinink. 2008. Single walled carbon nanotubes (SWCNT) affect cell physiology and cell architecture. *J Mater Sci Mater Med* 19 (4):1523-7.

Kido, T., Y. Morimoto, E. Asonuma, K. Yatera, A. Ogami, T. Oyabu, I. Tanaka, and M. Kido. 2008. Chrysotile asbestos causes AEC apoptosis via the caspase activation in vitro and in vivo. *Inhal Toxicol* 20 (3):339-47.

Kisin, E. R., A. R. Murray, M. J. Keane, X. C. Shi, D. Schwegler-Berry, O. Gorelik, S. Arepalli, V. Castranova, W. E. Wallace, V. E. Kagan, and A. A. Shvedova. 2007. Single-walled carbon nanotubes: geno- and cytotoxic effects in lung fibroblast V79 cells. *J Toxicol Environ Health A* 70 (24):2071-9.

Lam, C., J. H. James, R. McCluskey, and R. Hunter. 2004. Pulmonary toxicity of single-wall carbon nanotubes in mice 7 and 90 days after intratracheal instillation. *Toxicol. Sci.* 77:126-134.

Lanone, S., and J. Boczkowski. 2006. Biomedical applications and potential health risks of nanomaterials: molecular mechanisms. *Curr. Mol. Med.* 6:651-663.

Li, J. G., W. X. Li, J. Y. Xu, X. Q. Cai, R. L. Liu, Y. J. Li, Q. F. Zhao, and Q. N. Li. 2007. Comparative study of pathological lesions induced by multiwalled carbon nanotubes

in lungs of mice by intratracheal instillation and inhalation. *Environ Toxicol* 22 (4):415-21.

Li, J. M., and A. M. Shah. 2002. Intracellular localization and preassembly of the NADPH oxidase complex in cultured endothelial cells. *J. Biol. Chem.* 277:19952-19960.

Lu, J., M. J. Keane, T. Ong, and W. E. Wallace. 1994. In vitro genotoxicity studies of chrysotile asbestos fibers dispersed in simulated pulmonary surfactant. *Mutat Res* 320 (4):253-9.

Manna, S. K., S. Sarkar, J. Barr, K. Wise, E. V. Barrera, O. Jejelowo, A. C. Rice-Ficht, and G. T. Ramesh. 2005. Single-walled carbon nanotube induces oxidative stress and activates nuclear transcription factor-kappaB in human keratinocytes. *Nano Lett* 5 (9):1676-84.

Mohr, S., G. Keith, and B. Rihn. 2005. [Asbestos and malignant pleural mesothelioma: molecular, cellular and physiopathological aspects]. *Bull Cancer* 92 (11):959-76.

Monteiro-Riviere, N. A., A. O. Inman, Y. Y. Wang, and R. J. Nemanich. 2005. Surfactant effects on carbon nanotube interactions with human keratinocytes. *Nanomedicine* 1 (4):293-9.

Monteiro-Riviere, N., and A. Inman. 2006. Challenges for assessing carbon nanomaterials toxicity to the skin. *Carbon* 44:1070-1078.

Monteiro-Riviere, N., R. Nemanich, A. Inman, Y. Wang, and J. Riviere. 2005. Multi-walled carbon nanotube interactions with human epidermal keratinocytes. *Toxicol. Letters* 155:377-384.

Muller, J., F. Huaux, N. Moreau, P. Misson, J. F. Heilier, M. Delos, M. Arras, A. Fonseca, J. B. Nagy, and D. Lison. 2005. Respiratory toxicity of multi-wall carbon nanotubes. *Toxicol Appl Pharmacol* 207 (3):221-31.

Mutsaers, S. E. 2004. The mesothelial cell. *Int J Biochem Cell Biol* 36 (1):9-16.

Nardone, L., and S. Andrews. 1979. Cell line A549 as a model of the type II pneumocyte. Phospholipid biosynthesis from native and organometallic precursors. *Biochim Biophys Acta* 573:276-295.

Nel, A., T. Xia, L. Madler, and N. Li. 2006. Toxic potential of materials at the nanolevel. *Science* 311 (5761):622-7.

Nymark, P., P. M. Lindholm, M. V. Korpela, L. Lahti, S. Ruosaari, S. Kaski, J. Hollmen, S. Anttila, V. L. Kinnula, and S. Knuutila. 2007. Gene expression profiles in asbestos-exposed epithelial and mesothelial lung cell lines. *BMC Genomics* 8:62.

Ovrevik, J., M. Refsnes, E. Namork, R. Becher, D. Sandnes, P. E. Schwarze, and M. Lag. 2006. Mechanisms of silica-induced IL-8 release from A549 cells: Initial kinase-activation does not require EGFR activation or particle uptake. *Toxicology*.

Ryter, S. W., and A. M. Choi. 2005. Heme oxygenase-1: redox regulation of a stress protein in lung and cell culture models. *Antioxid Redox Signal* 7 (1-2):80-91.

Sayes, C. M., F. Liang, J. L. Hudson, J. Mendez, W. Guo, J. M. Beach, V. C. Moore, C. D. Doyle, J. L. West, W. E. Billups, K. D. Ausman, and V. L. Colvin. 2006. Functionalization density dependence of single-walled carbon nanotubes cytotoxicity in vitro. *Toxicol Lett* 161 (2):135-42.

Shvedova, A. A., E. R. Kisin, R. Mercer, A. R. Murray, V. J. Johnson, A. I. Potapovich, Y. Y. Tyurina, O. Gorelik, S. Arepalli, D. Schwegler-Berry, A. F. Hubbs, J. Antonini, D. E. Evans, B. K. Ku, D. Ramsey, A. Maynard, V. E. Kagan, V. Castranova, and P. Baron. 2005. Unusual inflammatory and fibrogenic pulmonary responses to single-walled carbon nanotubes in mice. *Am J Physiol Lung Cell Mol Physiol* 289 (5):L698-708.

Smart, S;, A. Cassady, G. Lu, and D. Martin. 2006. The biocompatibility of carbon nanotubes. *Carbon* 44:1034-1047.

Soto, K., K. M. Garza, and L. E. Murr. 2007. Cytotoxic effects of aggregated nanomaterials. *Acta Biomater*.

Sumimoto, H., K. Miyano, and R. Takeya. 2005. Molecular composition and regulation of the Nox family NAD(P)H oxidases. *Biochem Biophys Res Commun* 338 (1):677-86.

Taille, C., J. El-Benna, S. Lanone, M. C. Dang, E. Ogier-Denis, M. Aubier, and J. Boczkowski. 2004. Induction of Heme Oxygenase-1 Inhibits NAD(P)H Oxidase Activity by Down-regulating Cytochrome b558 Expression via the Reduction of Heme Availability. *J Biol Chem* 279 (27):28681-8.

Takagi, A., A. Hirose, T. Nishimura, N. Fukumori, A. Ogata, N. Ohashi, S. Kitajima, and J. Kanno. 2008. Induction of mesothelioma in p53+/- mouse by intraperitoneal application of multi-wall carbon nanotube. *J Toxicol Sci* 33 (1):105-16.

Tian, F., D. Cui, H. Schwarz, G. G. Estrada, and H. Kobayashi. 2006. Cytotoxicity of single-wall carbon nanotubes on human fibroblasts. *Toxicol In Vitro* 20 (7):1202-12.

Warheit, D. B., B. R. Laurence, K. L. Reed, D. H. Roach, G. A. Reynolds, and T. R. Webb. 2004. Comparative pulmonary toxicity assessment of single-wall carbon nanotubes in rats. *Toxicol Sci* 77 (1):117-25.

Wick, P., P. Manser, L. K. Limbach, U. Dettlaff-Weglikowska, F. Krumeich, S. Roth, W. J. Stark, and A. Bruinink. 2007. The degree and kind of agglomeration affect carbon nanotube cytotoxicity. *Toxicol Lett* 168 (2):121-31.

Worle-Knirsch, J. M., K. Pulskamp, and H. F. Krug. 2006. Oops they did it again! Carbon nanotubes hoax scientists in viability assays. *Nano Lett* 6 (6):1261-8.

TABLES

Table 1 Characterization of surface functional groups present on MWCNT using a Knudsen flow reactor.

Gas [gas-phase probe molecules]	**$N(CH_3)_3$** [acidic sites]	**HCl** [basic sites]	**CF_3COOH** [basic sites]	**NH_2OH** [carbonyl functions]	**O_3** [oxidizable sites]	**NO_2** [oxidizable sites]
no/mg[a]	$3.0 \cdot 10^{15}$	$8.1 \cdot 10^{16}$	$2.4 \cdot 10^{16}$	$2.4 \cdot 10^{17}$	$3.9 \cdot 10^{18}$	$1.2 \cdot 10^{16}$
no/cm^{2}[b]	$1.4\ 10^{12}$	$3.7\ 10^{13}$	$1.1\ 10^{13}$	$1.1\ 10^{14}$	$1.8\ 10^{15}$	$5.3\ 10^{12}$
ML[c]	0.28%	7.4%	2.2%	22%	360%	1.1%

Results are expressed as indicated in footnotes a, b and c and using a BET surface of 219.2 m^2/g.

[a] number of probe molecules taken up per mg of deposited nanoparticles

[b] number of probe molecules taken up per square cm of MWCNT (no/cm^2)

[c] number or fraction of formal monolayer (ML) of reacted probe gas using an average of $5x10^{14}$ molecules cm^{-2} as one formal ML.

Table 2

	MWCNT agglomerate area (μm^2)/field	MWCNT agglomerate number/field
A549 (DPL)	**16,64 ± 1,50**	**154,50 ± 7,23**
(EtOH)	**20,11 ± 2,01**	**99,60 ± 5,15 #**
(PBS)	**31,08 ± 2,20 ***	**155,40 ± 10,11**
Met5A (DPL)	**14,29 ± 0,93**	**42,80 ± 2,09**

Quantification of agglomerates formed after 48 hr incubation of A549 or MeT5A cells with 100 μg/ml of MWCNT suspended in DPL, EtOH, or PBS. Results are means ± SEM of the values obtained for 10 fields. * $p<0.05$ vs DPL and EtOH. #$p<0.05$ vs DPL and PBS.

LEGENDS TO FIGURES

Figure 1

Transmission electronic microscopy (TEM) images of MWCNT powder (Panel A) or in suspension (Panel B) in the different media (1: DPL; 2: EtOH; 3: PBS).

Figure 2

Representative optical microscopy images of cells exposed to the different particles.

Panel A: A459 cells exposed for 48 hr to medium alone (Panel 1), 100 μg/ml CB (Panel 2), chrysotile (Panel 3), crocidolite fibers (Panel 4), or MWCNT suspended in DPL, EtOH, or PBS (Panel 5, 6 and 7 respectively). Magnification: x 20.

Panel B: MeT5A cells exposed for 48 hr to medium alone (Panel 1), 100 μg/ml CB (Panel 2), crocidolite (Panel 3) or MWCNT suspended in DPL (Panel 4). Magnification: x 20.

Figure 3

Cell viability assessed by MTT assay.

Panel A: Viability, expressed as a % of control cell values, of A549 cells after 6, 24, 48 or 72 hr exposure to 100 μg/ml CB, chrysotile, crocidolite or 0.1 to 100 μg/ml MWCNT in 1% DPL, EtOH, or PBS.

Panel B: Viability, expressed as a % of control cell values, of MeT5A cells after 48-hr exposure to 100 μg/ml CB, chrysotile, crocidolite or 0.1 to 100 μg/ml MWCNT in 1% DPL. *$p<0.05$ *vs* control condition.

Figure 4

DNA content.

Panel A: DNA content, expressed as a % of control cell values, of A549 cells after 24, 48 or

72 hr exposure to 100 μg/ml CB, crocidolite or 100 μg/ml MWCNT in 1% DPL, EtOH, or PBS.

Panel B: DNA content, expressed as a percentage of control cell values, of MeT5A cells after 48 hr exposure to 100 μg/ml CB, crocidolite or 100 μg/ml MWCNT in 1% DPL. *p<0.05 *vs* control condition.

Figure 5

Apoptosis assessment.

Panels A and B. Representative microscopic images of A549 cells (Panel A) and quantification of DAPI-positive cells (Panel B), after exposure of cells to 100 μg/ml nanomaterials for 72 hr.

Panels C and D. Representative microscopic images of MeT5A cells (Panel C) and quantification of DAPI-positive cells (Panel D), after exposure of cells to 100 μg/ml nanomaterials for 72 hr. Magnification x60. *p<0.05 vs control.

Figure 6

DNA laddering.

Panels A and B. Representative image for DNA laddering experiments in A549 (Panel A) and MeT5A (Panel B) cells exposed for 72 hr to 0% FCS (lane 1), 1% DPL (lane 2), 100 μg/ml crocidolite (lane 3), MWCNT in 1% DPL (lane 4) or etoposide used as positive control (lane 5).

Figure 7

Representative transmission electronic microscopy (TEM) images of A459 cells exposed for 48 hr to 100 μg/ml of culture medium alone (1), 100 μg/ml CB (2), chrysotile (3), crocidolite

(4), or MWCNT in DPL (5), EtOH (6), or PBS (7).

Figure 1

A

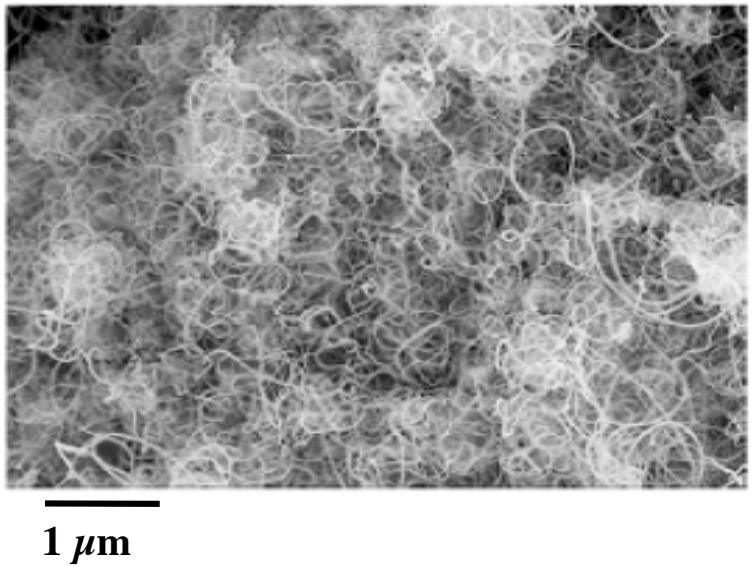

B

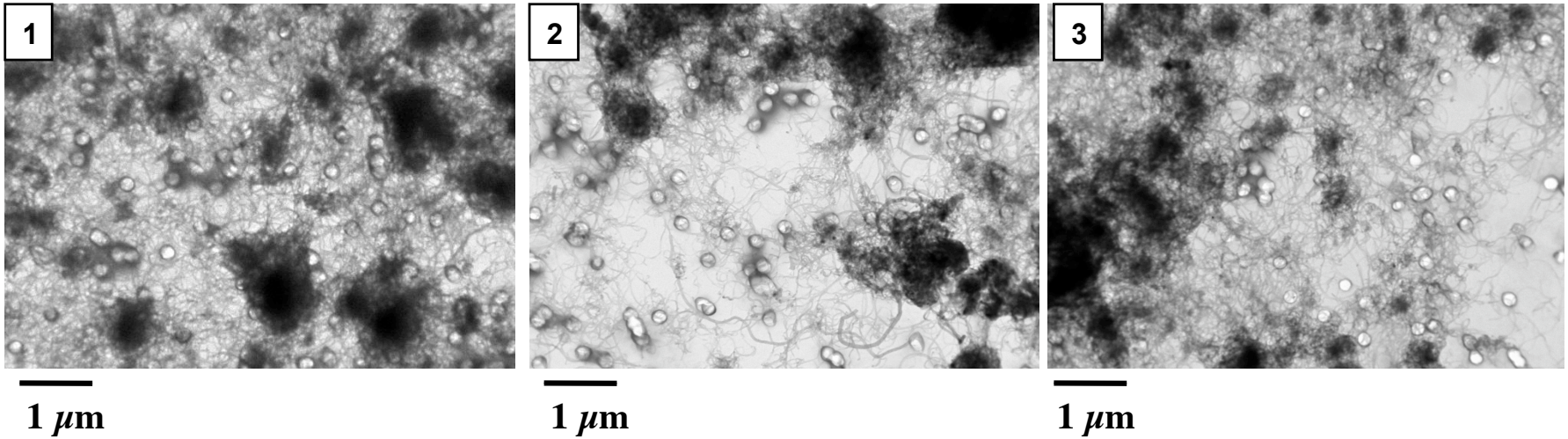

Figure 2

A

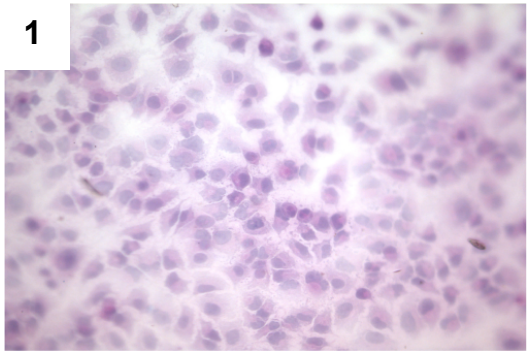

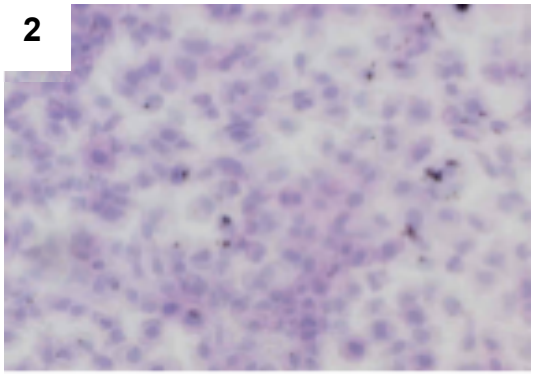

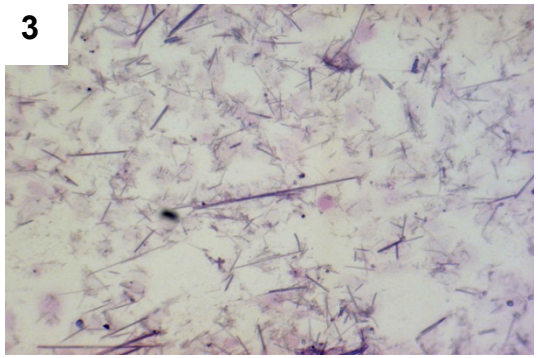

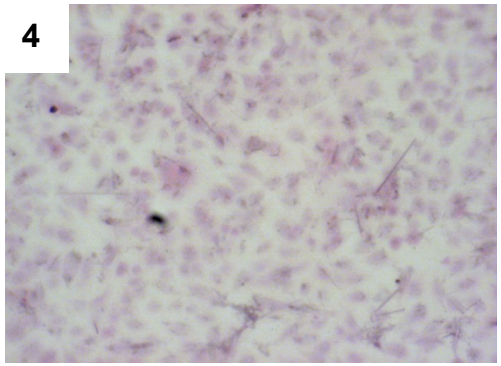

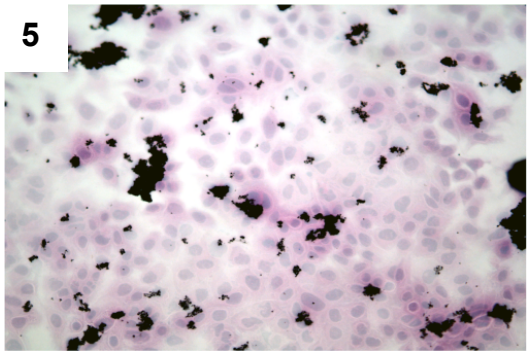

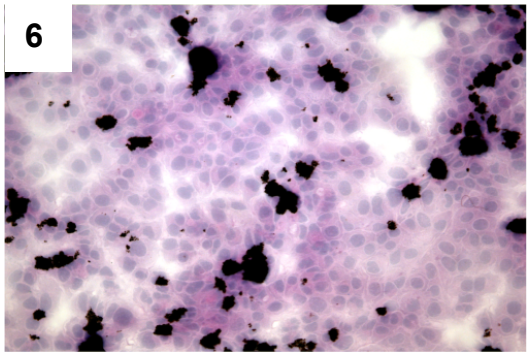

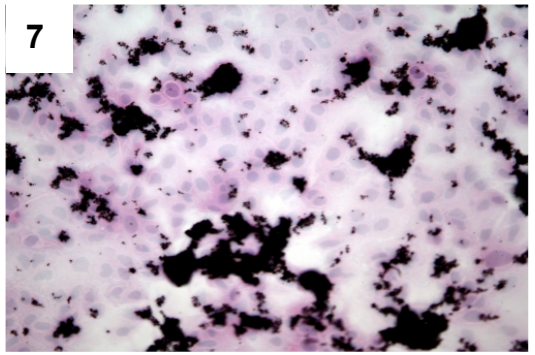

Figure 2

B

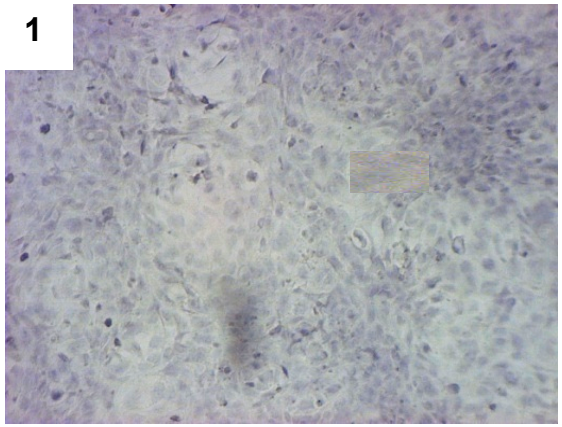

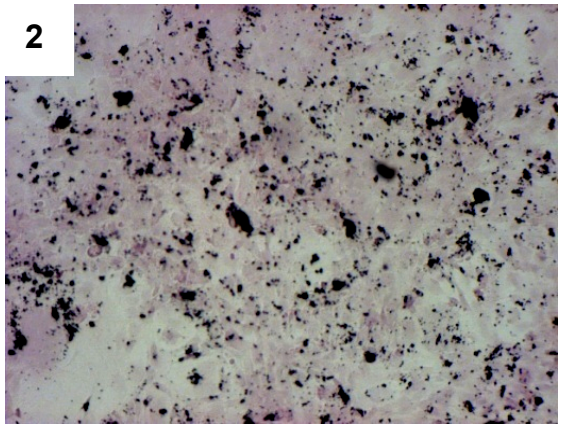

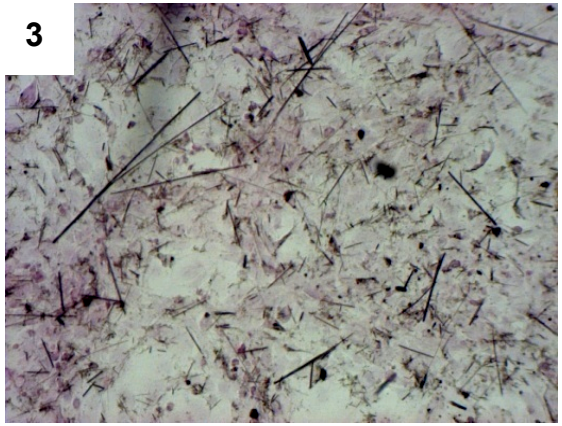

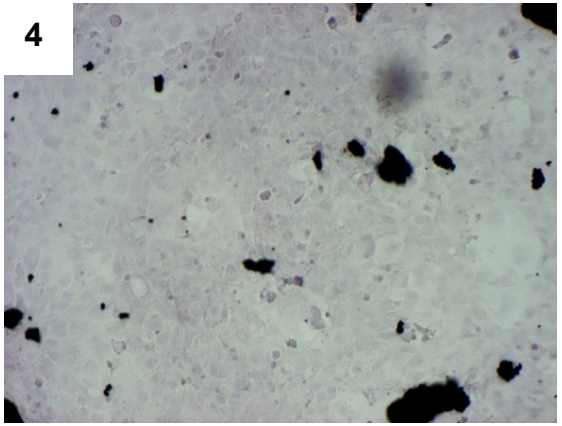

Figure 3

A

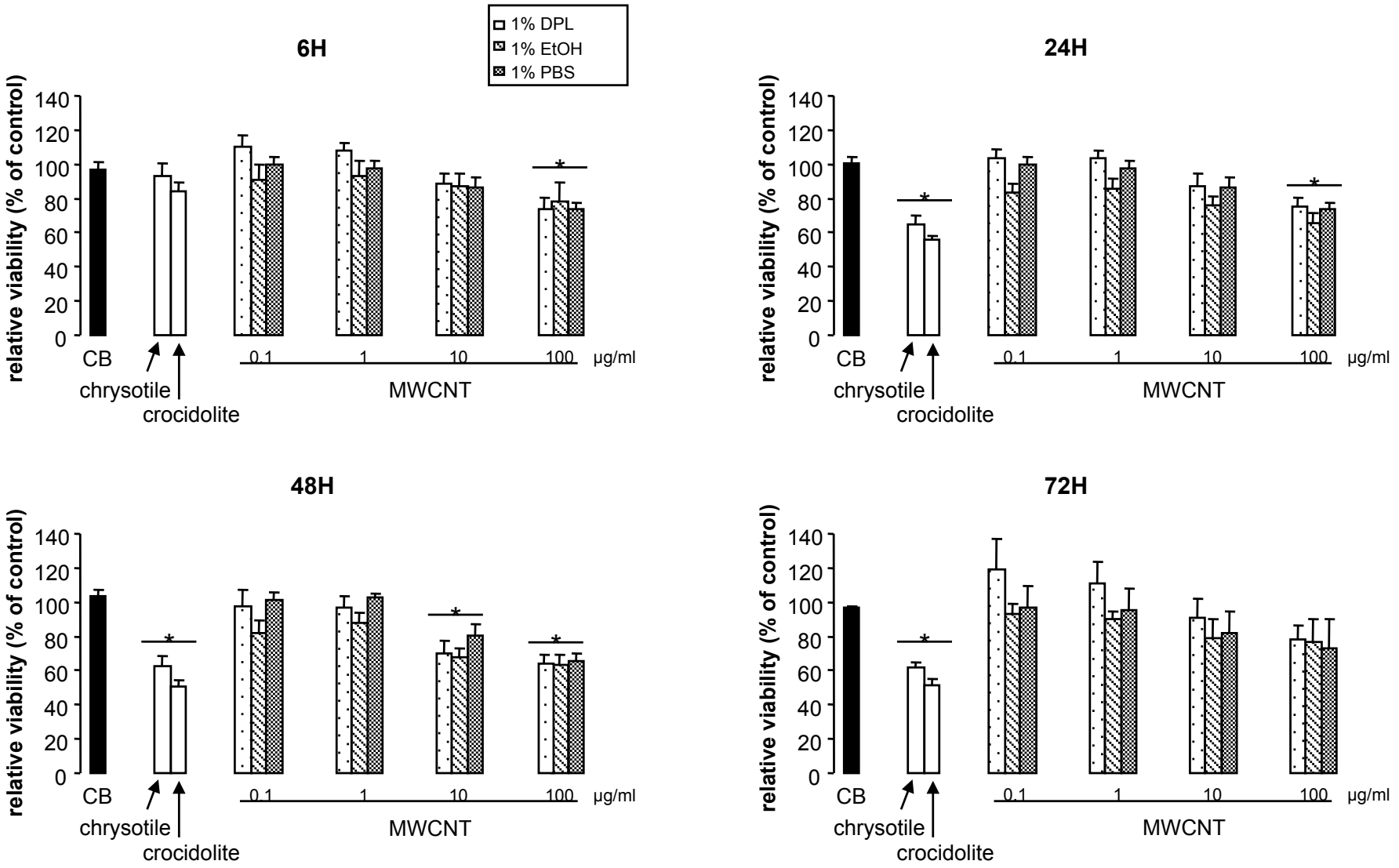
6H
24H
48H
72H
1% DPL
1% EtOH
1% PBS
relative viability (% of control)
0
20
40
60
80
100
120
140
CB
chrysotile
crocidolite
0.1
1
10
100
µg/ml
MWCNT
*

Figure 3

B

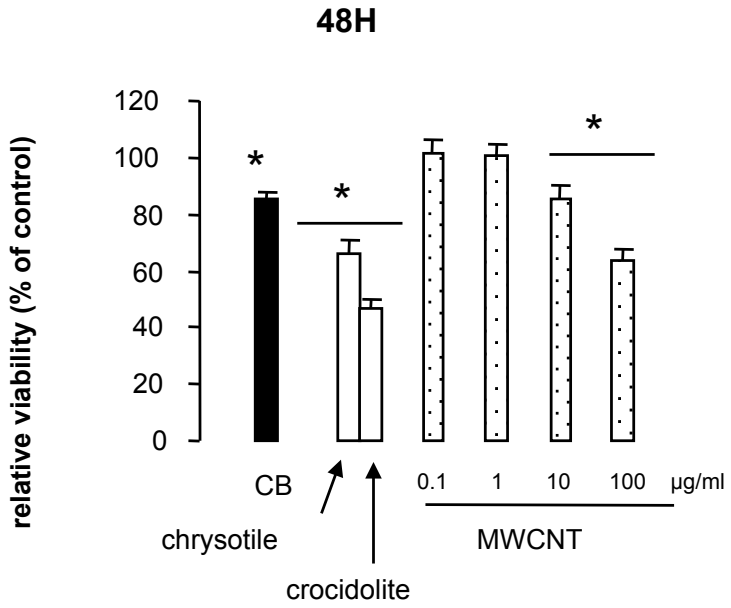
48H
relative viability (% of control)
120
100
80
60
40
20
0
*
*
*
CB
0.1
1
10
100
µg/ml
chrysotile
MWCNT
crocidolite

Figure 4

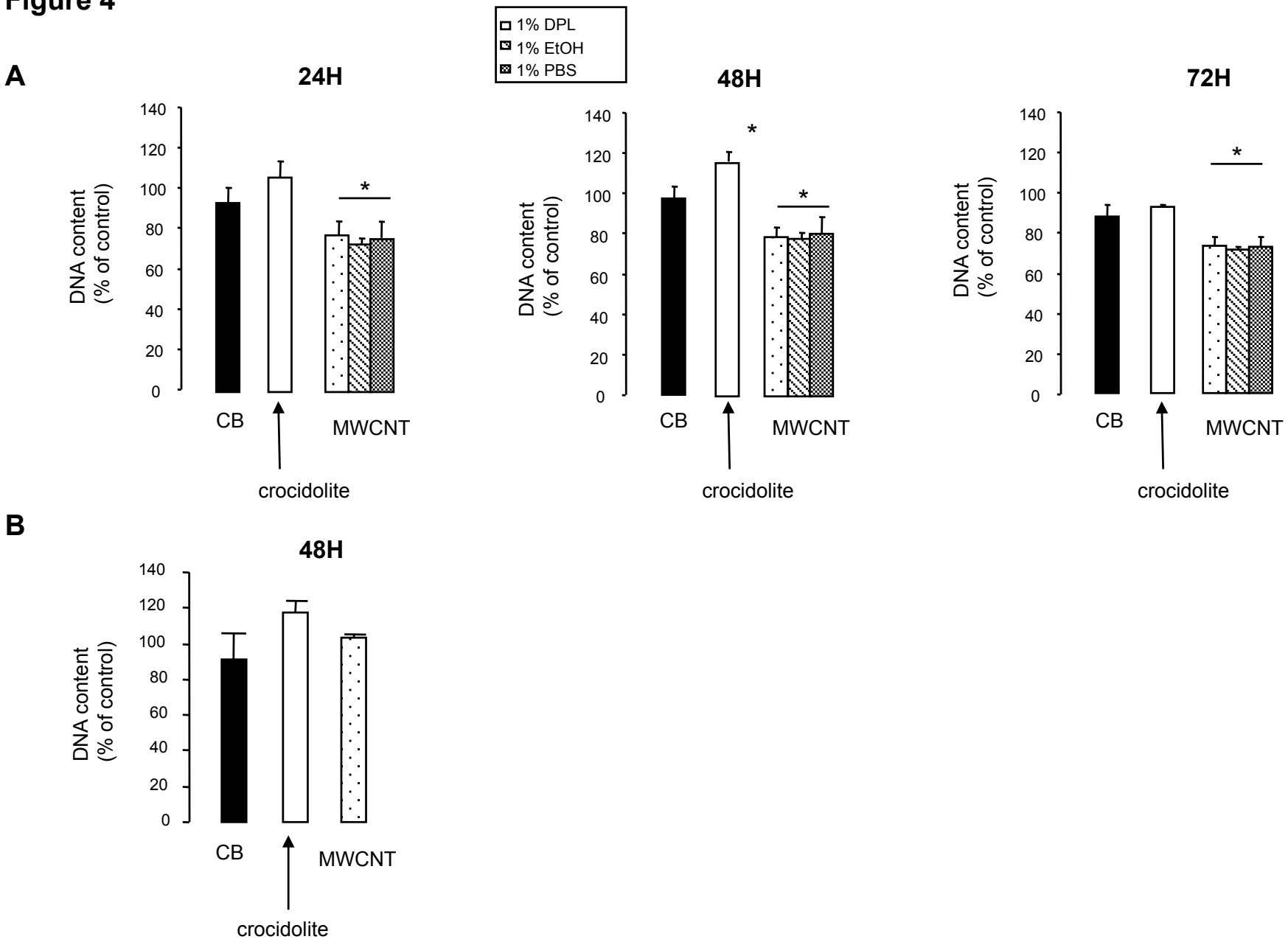
A
24H
48H
72H
1% DPL
1% EtOH
1% PBS
DNA content
(% of control)
140
120
100
80
60
40
20
0
*
CB
MWCNT
crocidolite
B
48H
DNA content
(% of control)
CB
MWCNT
crocidolite

Figure 5

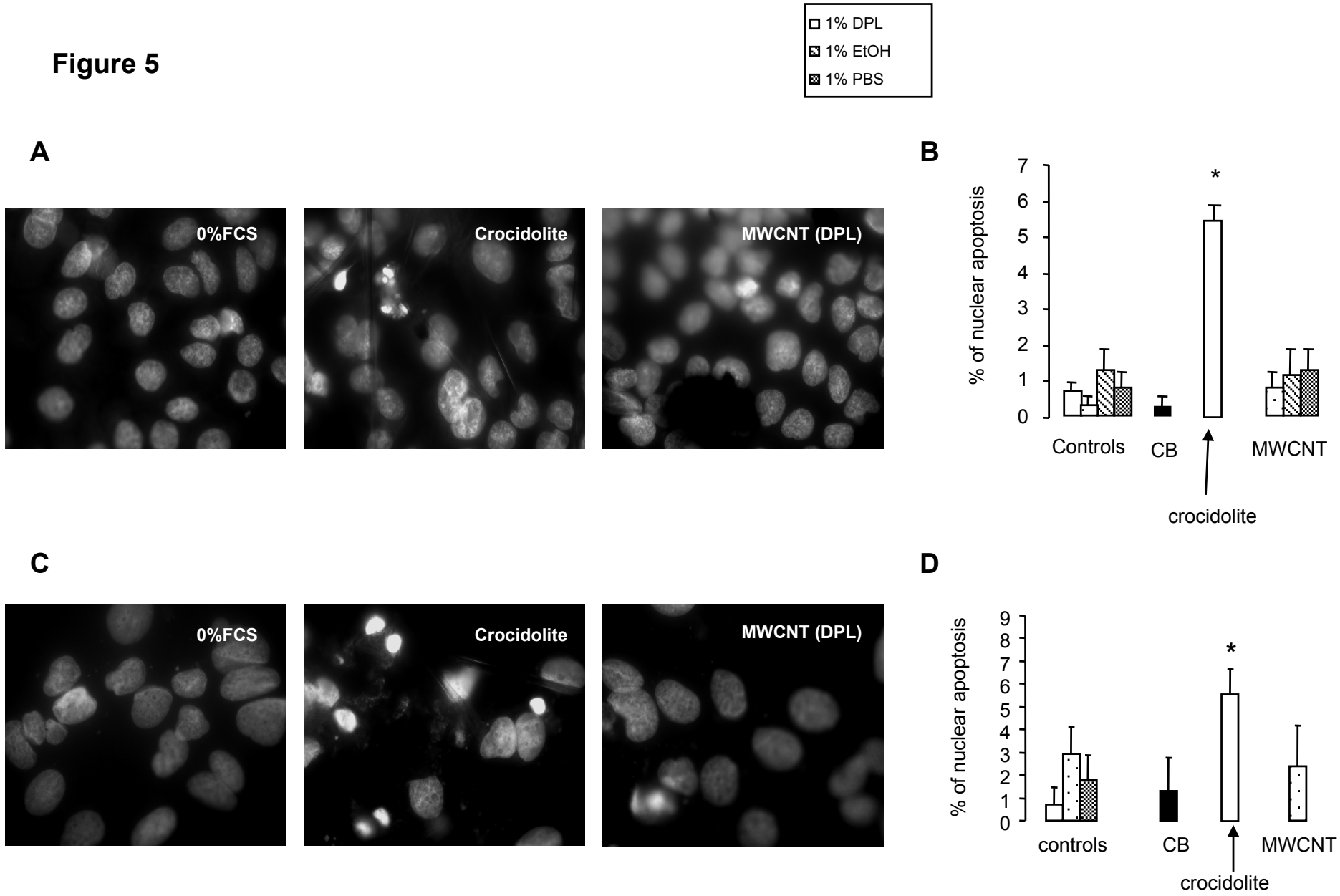
1% DPL
1% EtOH
1% PBS
A
0%FCS
Crocidolite
MWCNT (DPL)
B
% of nuclear apoptosis
0
1
2
3
4
5
6
7
*
Controls
CB
MWCNT
crocidolite
C
0%FCS
Crocidolite
MWCNT (DPL)
D
% of nuclear apoptosis
0
1
2
3
4
5
6
7
8
9
*
controls
CB
MWCNT
crocidolite

Figure 6

A

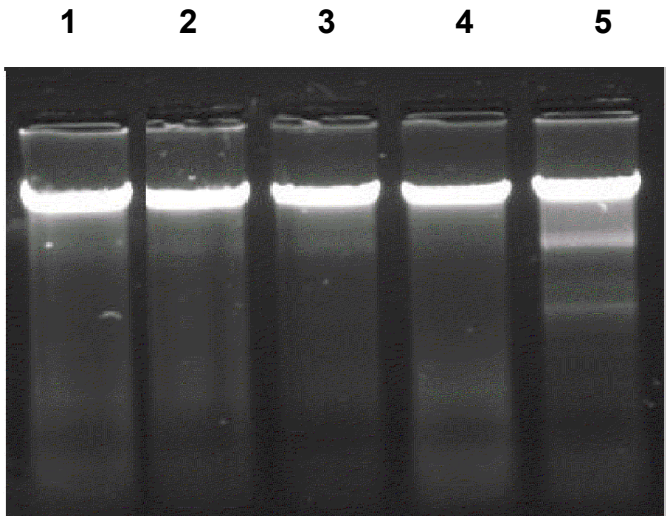

B

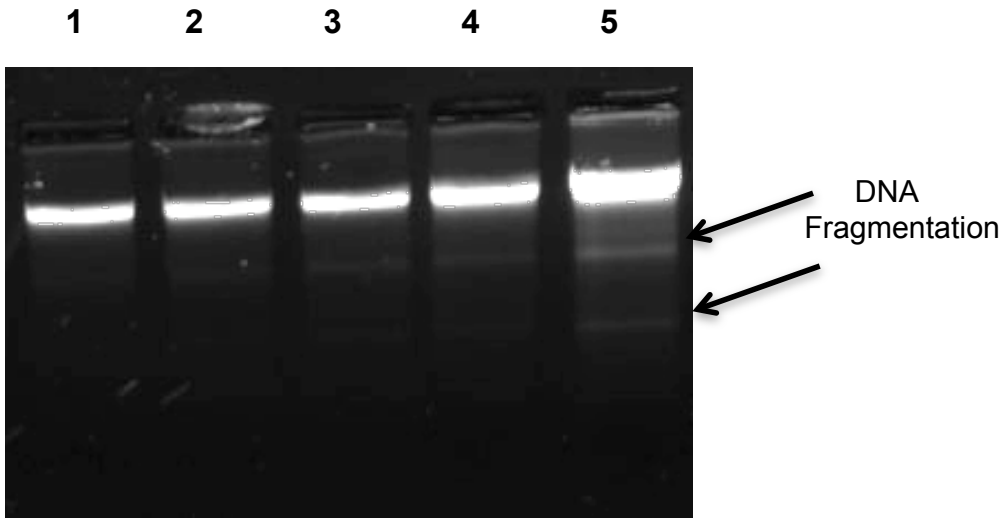

Figure 7

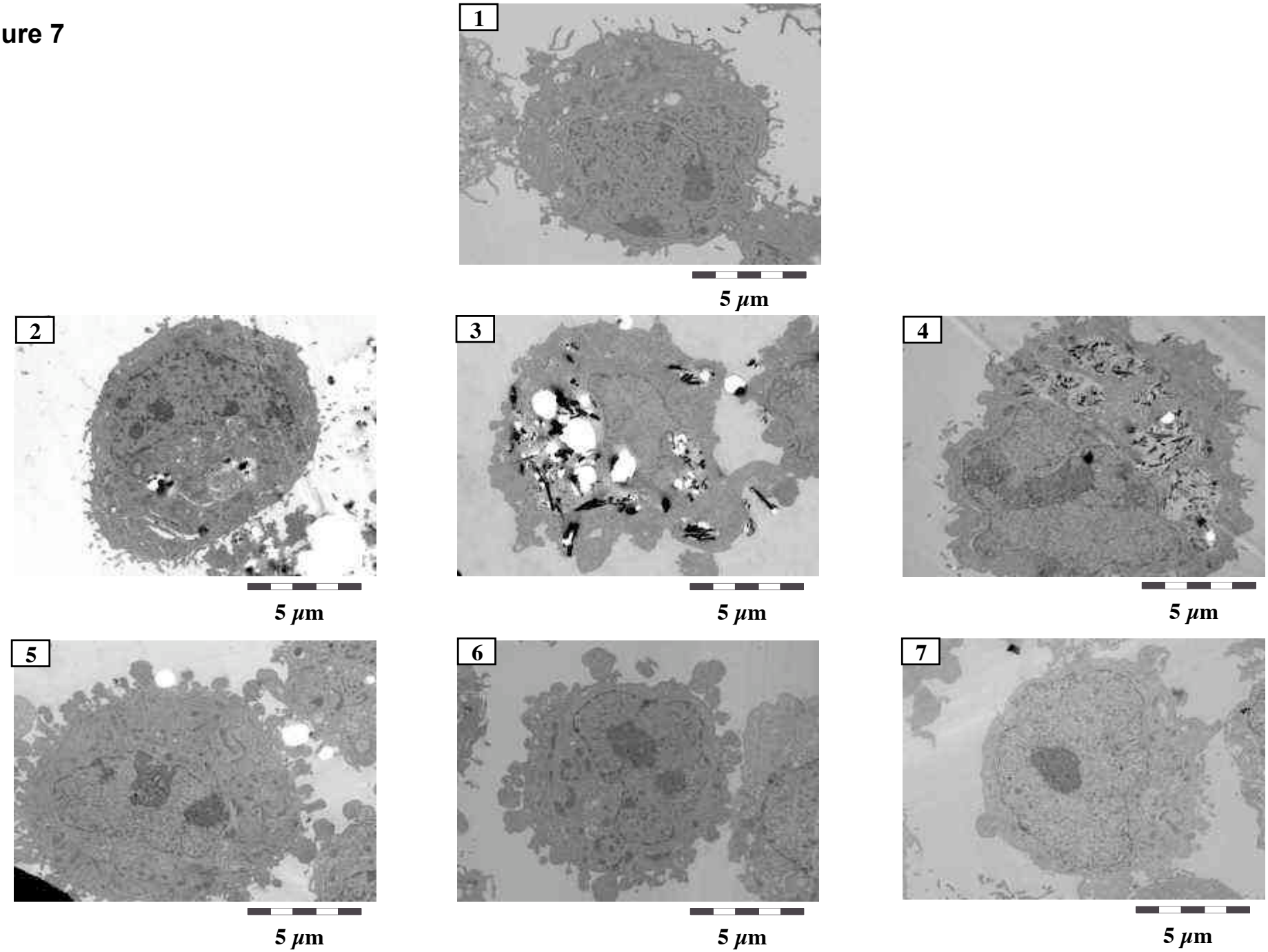

Table 1

Gas [gas-phase probe molecules]	$N(CH_3)_3$ [acidic sites]	HCl [basic sites]	CF_3COOH [basic sites]	NH_2OH [carbonyl functions]	O_3 [oxidizable sites]	NO_2 [oxidizable sites]
MWCNT	$6.0 \cdot 10^{13}$	$1.6 \cdot 10^{15}$	$4.9 \cdot 10^{14}$	$4.7 \cdot 10^{15}$	$7.8 \cdot 10^{16}$	$2.3 \cdot 10^{14}$

Table 2

	MWCNT aggregate area (μm^2)/field	MWCNT aggregate number/field
A549 (DPL)	16,64 ± 1,50	154,50 ± 7,23
(EtOH)	20,11 ± 2,01	99,60 ± 5,15 #
(PBS)	31,08 ± 2,20 *	155,40 ± 10,11
Met5A (DPL)	14,29 ± 0,93	42,80 ± 2,09